Position Sensors Fault Tolerant Control System in BLDC Motors

A. Tashakori and M. Ektesabi

***Abstract*—Developing of fault tolerant control systems (FTCS's) for permanent magnet Brushless DC (BLDC) motor drives to diagnose and handle various faults have been of the research concentrations in the last decade. In this paper a novel fault diagnosis algorithm for position sensors (Hall Effect sensors) failure of the BLDC motor is presented. Fault detection and identification of Hall Effect sensors are based on sensors signals and Discrete Fourier Transform (DFT) analysis of the BLDC motor line voltages in the proposed fault diagnosis system. BLDC motor behaviour is analysed under various Hall Effect sensor faults through a validated simulation model. An expert system is developed to diagnose Hall Effect sensors faults in the BLDC motor by analysing the simulation results under different fault conditions. Correct performance of the proposed fault diagnosis system is proven through experimental data analysis. A simple technique is discussed to generate the commutation signal of the faulty position sensor and maintain operation of the BLDC motor in post-fault condition. The proposed fault tolerant control system is simple, does not need excessive computations and can be executed with the main control program of the BLDC motor on a single chip micro-controller.**

***Index Terms*—BLDC motor, Hall Effect sensor failure, Fault tolerant control systems.**

I. Introduction

BLDC motors have been popular in various industrial applications in the last four decades. The BLDC motor is a DC motor type that has no brushes; therefore commutation is done electronically according to the permanent magnet rotor position. BLDC motors have higher efficiency, faster dynamic response (permanent magnet rotor), operate in higher speed ranges and need less maintenance in comparison to the conventional brushed DC motors; however they are more costly (high price of permanent magnet materials) and have more complex control techniques.

Correct commutation and control of BLDC motors depend on the exact position detection of rotor. Sensors such as optical encoders, for high resolution applications, and Hall Effect sensors, for low resolution applications, are normally used to detect position of the permanent magnet rotor [1]. Rotor position detection techniques in sensorless control drives of the BLDC motor are mainly based on back-EMF sensing, back-EMF integration, free-wheeling diode conduction of the unexcited phase, flux linkage of motor, and third-harmonic analysis of back-EMF [2].

Manuscript is received on October 01, 2013; revised on February 14, 2014.

A. Tashakori is a PhD candidate at the Faculty of Science, Engineering and Technology, Swinburne University of Technology, Melbourne, VIC 3101 Australia, e-mail: atashakoriabkenar@swin.edu.au.

M. Ektesabi is a senior lecturer at the Faculty of Science, Engineering and Technology, Swinburne University of Technology, Melbourne, VIC 3101 Australia.

Reduction of the BLDC motor manufacturing cost, the motor maintenance and possibility of the motor malfunctions due to failure or unbalanced positioning of sensors are advantages of sensorless control techniques; however difficulties of back-EMF sensing at low speeds and transient time, complexity of rotor detection algorithms and discontinuous response due to high commutation rates are the main drawbacks of sensorless techniques [3]. A novel FTCS for position sensors failure of the BLDC motor has been proposed by authors to increase reliability of the motor drives that using sensors for rotor position detection [1]. This paper is an extended research work of the reported paper by authors that effectiveness of the proposed position sensor fault diagnosis system is validated by experimental results.

The presented position sensor FTCS in this paper is proposed for three phase star connected permanent magnet BLDC motors with the inbuilt Hall Effect sensors. Four-phase, five-phase and six-phase BLDC motors are not in the scope of this paper, however they can be considered as potential research studies in future. Schematic diagram of a three phase, 4 poles, star connected BLDC motor drive is shown in Fig. 1.

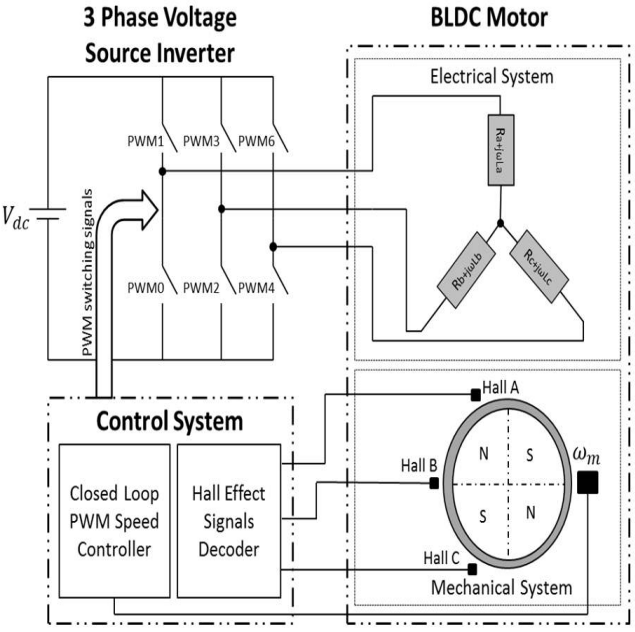

Fig. 1. Schematic diagram of a three phase BLDC motor drive

Hall Effect sensors detect position of the permanent magnet rotor based on Hall Effect theory. They are embedded at non-rotating end of the BLDC motor with 120 electrical

degree phase difference to detect the rotor position. Hall Effect sensor's output is high (logic '1') or low (logic '0') as the rotor magnetic poles N or S passes near the sensor. Therefore output of each sensor is high for 180 electrical degree and is low for the next 180 electrical degree with respect to the rotor position during one full electrical rotation of the BLDC motor. Correct voltage space vectors for switching of the three phase Voltage Source Inverter (VSI) drive of the BLDC motor are chosen by decoding Hall Effect signals. Ideal phase currents, back-EMF and commutation (Hall Effect) signals are shown in Fig.2.

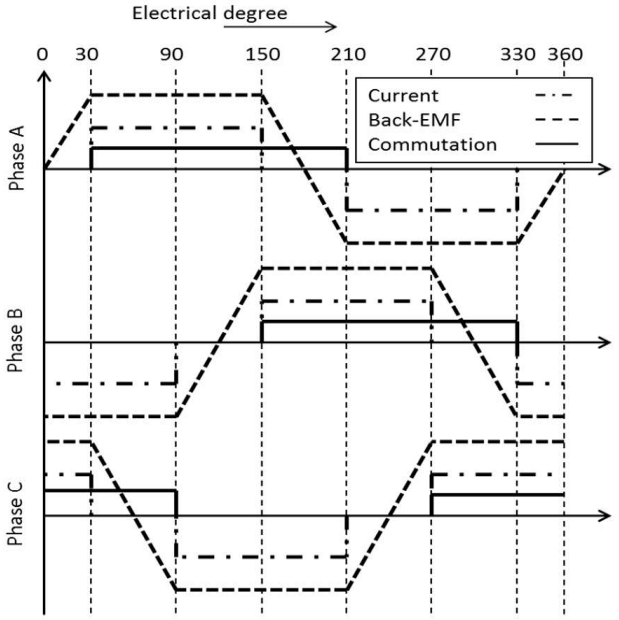

Fig. 2. Ideal waveforms of a three phase BLDC motor

Since the voltage space vectors are chosen by decoding of the Hall Effect signals to drive the VSI; any failure of Hall Effect sensor effects directly on the applied voltages to the BLDC motor and degrades the motor performance. Implementing FTCS's increase reliability of the electric motor drives in post-fault detection. Fault tolerant control systems mainly are responsible to detect and identify the fault, isolate the faulty section and take the appropriate remedial action to keep the system working with the maximum possible efficiency in the post-fault condition [4].

Signal analysis, model based and knowledge based methods are the main techniques for fault diagnosis in the BLDC motor drives [5]. In the signal analysis based methods, fault is detected and identified through comparison of the BLDC motor signals with the ideal situation. Therefore there is no need for an accurate dynamic model of the motor. Signal analysis fault diagnosis methods are generally slower than other two methods. Fault diagnosis in model based methods is quite fast and can be used for online fault detection; however the exact mathematical model of the BLDC motor is needed. Model based observers are popularly used in fault diagnosis systems; however fault detection residuals are influenced not only by system faults but also by disturbances and model uncertainties [6]. Since uncertainties, disturbances or noise in system are unknown and cannot be modelled mathematically; therefore there is always a difference between the mathematical model results and actual system performance that can generates false fault detections in model based systems [7]. In expert systems, fuzzy or neural network controllers are developed based on the knowledge of system [5]. The knowledge is collected and analysed either through an experienced engineer with a thorough understanding of the system, or via comprehensive study of the system dynamics through a validated simulation model [4]. This paper presents a knowledge based fault diagnosis system based on signal analysis methods for Hall Effect sensor breakdown of the BLDC motor.

Flaws in the Hall Effect sensor's core due to corrosion, cracks, residual magnetic fields and core breakage; effect of temperature variations on the magnetic properties of the ferrite core; effect of mechanical shocks on orientation of the induced magnetic field in the sensor; and changes in the bias current of the sensor are main faults that may result in failure of Hall Effect sensors in the BLDC motors [8]. Unbalanced positioning of Hall Effect sensors inside the BLDC motor increases the low frequency harmonics in torque ripples and degrades the overall drive performance of the motor [9], however it does not in the position sensor failure and is not in the scope of this paper.

Few research works are reported on FTCS for Hall Effect sensor failure in the BLDC motors. Major possible sensor faults in the propulsion system of an interior-permanent-magnet-motor (IPMM)-based electric vehicle are discussed and remedial strategies are proposed [10]. Fault in position sensors are detected through difference between the calculated rotor angle and the actual rotor angle by a sensorless algorithm based on extended EMF in rotating reference frame. Shift to the sensorless control mode of permanent-magnet-motor is proposed as a remedial strategy to rectify the fault. Complexities of permanent magnet synchronous motor's sensorless control schemes and transition algorithms to sensorless mode are the main drawbacks of the proposed method. Behaviour of the BLDC motor under position sensors faults in lunar rover wheel application is analysed through simulation model [11]. Effects of Hall Effect sensor faults on switching signals of VSI and phase current waveforms are presented. However there is not any discussion on the simulation results, the fault diagnosis technique and remedial strategies in the mentioned paper.

An intelligent fault tolerant control system for Hall Effect sensor failure in the BLDC motors is presented in this paper. BLDC motor behaviour is analysed under various position sensor fault conditions on the next section. Hall Effect sensor fault diagnosis algorithm for the BLDC motor and a novel and simple remedial strategy to rectify the fault are presented and discussed on the following sections. Finally effectiveness of the proposed fault diagnosis algorithm is investigated through experiment.

II. BLDC motor behaviour analysis under Hall Effect sensor faults

To find an algorithm to detect and identify the faulty sensor, first it is necessary to study behaviour of the BLDC

motor under various position sensor faults through a validated simulation model. Therefore the BLDC motor drive using a closed loop digital Pulse Width Modulation (PWM) speed controller is modelled in Simulink. A low voltage three phase permanent magnet BLDC motor is used as a practical test rig to validate simulation model of the motor. Low voltage development board of microchip using PIC18F4231 micro-controller is programmed to control the BLDC motor. The control board has an in-built over current protection circuit and the inverter section consists of three half-bridge gate drivers using MOSFETs. High frequency PWM control signal is applied to all the switches of the inverter. Experimental test rig of the BLDC motor is shown in Fig. 3.

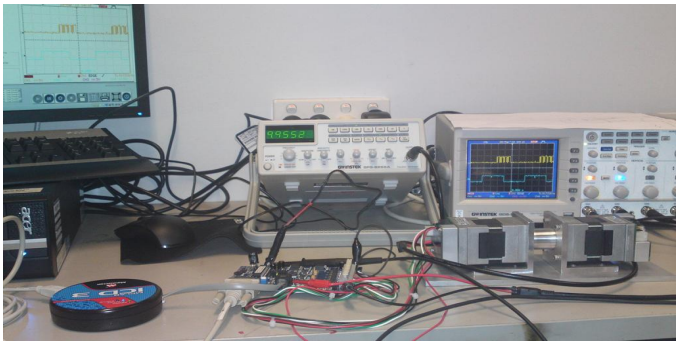

Fig. 3. Experimental test rig of the BLDC motor

The experimental BLDC motor specifications, given in Table I, have been used in the motor simulation model. The three phase VSI drive of the BLDC motor is simulated using MOSFET switches same as the experimental motor drive. Duty cycle of PWM signal is adjusted by a Proportional Integral (PI) controller based on speed error of the motor. An embedded code is written in Simulink model to generate the high frequency duty cycle controlled PWM signal [1].

TABLE I
SPECIFICATIONS OF THE EXPERIMENTAL BLDC MOTOR

Description	Value	Unit
DC voltage	24	V
Rated speed	3000	RPM
Rated Torque	0.28	$N.m$
Phase resistance	2.015	ohm
Phase inductance	4.60	mH
Inertia	4.43e-6	$kg.m^2$
Torque constant	0.069	$N.m/A$
Poles	8	-

Both the experimental motor and the simulation model of the BLDC motor are tested at 2000 RPM reference speed of controller under 0.1 N.m load torque. The phase A line voltage and its corresponding Hall Effect signal for the experimental BLDC motor and its simulation model are shown in Fig. 4. As can be seen in the figure, simulation results are in a good agreement with experimental data of the BLDC motor under the same operating condition that validates the simulated model of the motor.

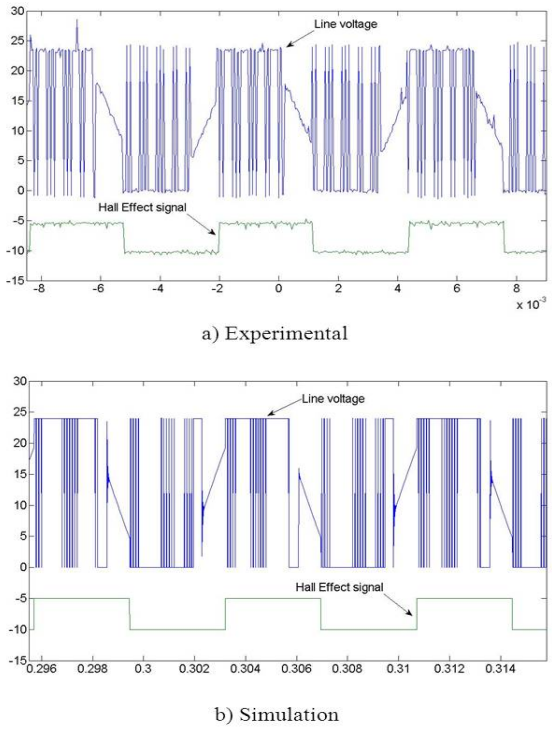

Fig. 4. Line voltage and corresponding Hall Effect signal of phase A of the BLDC motor

Hall Effect sensor faults are applied to the validated simulation model of the BLDC motor and output characteristics of the motor such as line voltages, speed and torque characteristics are analysed. Breakdown of a Hall Effect sensor is divided into two possible conditions based on the output signal of the sensor. Sensor's output is considered to be either constant high (logic '1'), sensor is short circuit, or constant low (logic '0'), sensor is open circuit [1]. Therefore sensor's signal does not change according to the rotor position. Behaviour of the BLDC motor is presented and discussed for both faulty conditions of the corresponding Hall Effect position sensor of phase A ($H_a = 0$ and $H_a = 1$).

A. Hall Effect signal is constant zero

Open circuit Hall Effect sensor fault $H_a = 0$ is applied to the validated BLDC motor model at $t = 0.5$ s, while the motor is running under healthy condition for 0.1 N.m torque load at 2000 RPM speed. Speed and torque characteristics of the BLDC motor for $H_a = 0$ fault condition are shown in Fig. 5. As is shown speed of the motor is unstable and electrical torque ripples amplitude is increased remarkably after fault occurrence.

Line voltages of the BLDC motor for $H_a = 0$ fault condition are shown in Fig. 6. Since the voltage of neutral point of the BLDC motor is neither provided by the manufacturer nor stable during high frequency PWM switching; therefore line voltages of the motor are sensed with respect to the negative terminal of the VSI DC link [1]. As can be seen Hall Effect sensor fault effect directly on the switching signals of the VSI

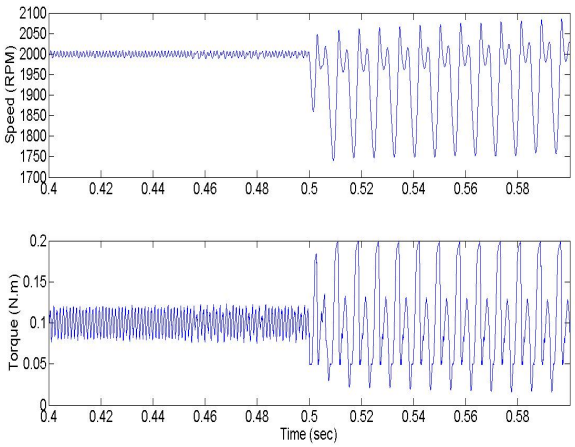

Fig. 5. Speed and torque characteristics of the BLDC motor for $H_a = 0$

and change pattern of the applied line voltage of the BLDC motor.

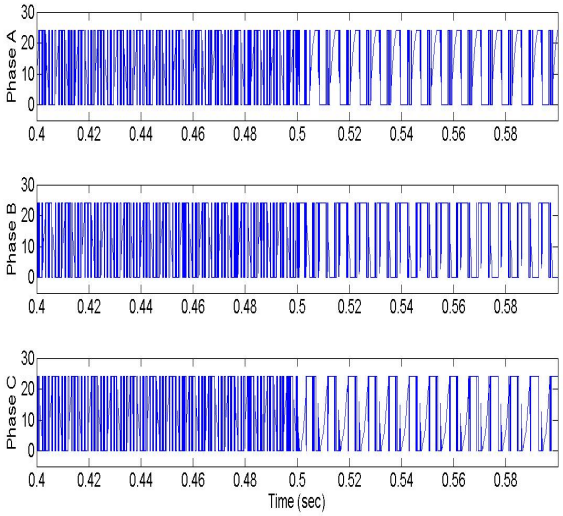

Fig. 6. Line voltages of the BLDC motor for $H_a = 0$

Various Hall Effect sensor faults are applied to the BLDC motor simulation model and effect of position sensor faults on the switching signals of VSI are summarized in Table II. Each Hall Effect sensor fault cause two switching signals of the VSI to be constant zero that can be interpreted as open circuit faults of two VSI switches at the same time. For instance under $H_a = 0$ fault condition, corresponding switching signals of PWM_1 and PWM_4 are constant zero (those switches are open circuit). Any VSI switching signals variations directly effect on the applied voltages to the BLDC motor, increases the torque ripples and degrade the motor performance.

B. Hall Effect signal is constant one

Short circuit Hall Effect sensor fault $H_a = 1$ is applied to the validated BLDC motor model at $t = 0.5$ s, while the motor is running under healthy condition for 0.1 N.m torque load at 2000 RPM speed. Speed and torque characteristics of the BLDC motor for $H_a = 1$ fault condition are similar to $H_a = 0$ fault condition. Torque ripples amplitude is increased and the BLDC motor is not stable after fault occurrence.

TABLE II
SENSORS FAULT EFFECT ON THE VSI SWITCHING SIGNALS

Fault type	Effected switching signals of the VSI	Switches status
$H_a = 0$	PWM_1 , PWM_4	Open
$H_a = 1$	PWM_5 , PWM_0	Open
$H_b = 0$	PWM_3 , PWM_0	Open
$H_b = 1$	PWM_1 , PWM_2	Open
$H_c = 0$	PWM_5 , PWM_2	Open
$H_c = 1$	PWM_3 , PWM_4	Open

Although speed and torque responses of the BLDC motor for $H_a = 1$ are similar to the ones for $H_a = 0$ fault condition; however affected switching signals of the VSI is different. Switching signals PWM_0 and PWM_5 are constant zero for $H_a = 1$ fault condition. Therefore applied voltages to the BLDC motor are totally different for $H_a = 1$ fault condition compare to the $H_a = 0$ fault. Line voltages of the BLDC motor for $H_a = 1$ fault condition are shown in Fig. 7.

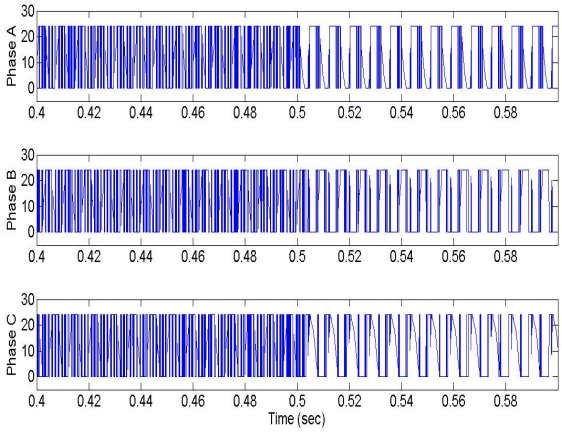

Fig. 7. Line voltages of the BLDC motor for $H_a = 1$

III. FAULT DIAGNOSIS

Hall Effect signals (commutation signals) of BLDC motor are either high or low according to the electrical degree position of permanent magnet rotor. Correct voltage space vectors are chosen according to the electrical position of rotor by decoding the commutation signals. Hall Effect signals and conducting switches of the VSI according to the permanent magnet rotor position are summarized in Table III.

There is no position of permanent magnet rotor that all three hall signals being one or zero at a same time. Addition of commutation signals are either one or two at any electrical angle position of the rotor. Therefore any failure of Hall

TABLE III
DECODING RULES OF COMMUTATION SIGNALS IN THE BLDC MOTORS

Rotor angle (Electrical degree)	H_a	H_b	H_c	Conducting switches
30-90	1	0	1	PWM_1 , PWM_2
90-150	1	0	0	PWM_1 , PWM_4
150-210	1	1	0	PWM_3 , PWM_4
210-270	0	1	0	PWM_3 , PWM_0
270-330	0	1	1	PWM_5 , PWM_0
330-30	0	0	1	PWM_5 , PWM_2

sensors changes value H_f introduced by (1) during one full electrical rotation of rotor.

$$H_f = H_a + H_b + H_c \tag{1}$$

If $H_f = 3$, it means that one of the position sensors is constant one and if $H_f = 0$, it means that one of the position sensors is constant zero. Fault detection time is less or equal to the time needed for one electrical rotation of rotor that is quite fast. Therefore Hall Effect sensors Fault Flag (HFF) is introduced for sensor fault detection as below,

- HFF is set '0' if $H_f = 1$ or $H_f = 2$;
- HFF is set '1' if $H_f = 3$;
- HFF is set '-1' if $H_f = 0$.

Hall Effect sensor fault is detected if HFF is not zero. However identification of faulty sensor is not possible through Hall Effect sensor Fault Flag. DFT analysis of line voltages of the BLDC motor is used for fault identification. In practice, line voltages of the BLDC motor is measured for specific interval of time and saved in memory of micro-controller. Then DFT of the saved measured line voltages are calculated by (2) and Spectral Energy Density (SED) of the computed frequency spectrum are determined by (3). SED difference of the measured line voltages between successive time intervals for constant speed and torque load are signature for identifying of faulty sensor [1].

$$V(f) = \sum_{n=0}^{N-1} V_n e^{-j2\pi k \frac{n}{N}} \qquad k = 0, 1, ..., N \tag{2}$$

$$E_m(f) = |V(f)|^2 \tag{3}$$

$$\varepsilon_m = E_m(f) - E_{m-1}(f) \tag{4}$$

Single-sided amplitude spectrum of phase A line voltage of the BLDC motor model for no fault and Hall Effect sensor faults of phase A ($H_a = 0$ and $H_a = 1$) are shown in Fig. 8. As can be seen high amplitude harmonics are added to the line voltage of phase A under faulty conditions compare to the healthy operation condition. Therefore energy densities of the voltage signals of the BLDC motor under position sensor faults condition are not same as the healthy operating condition. Calculated SED errors of the BLDC motor line voltages for Hall Effect sensor faults of $H_a = 0$ and $H_a = 1$ faults are given in Table IV and Table V, respectively.

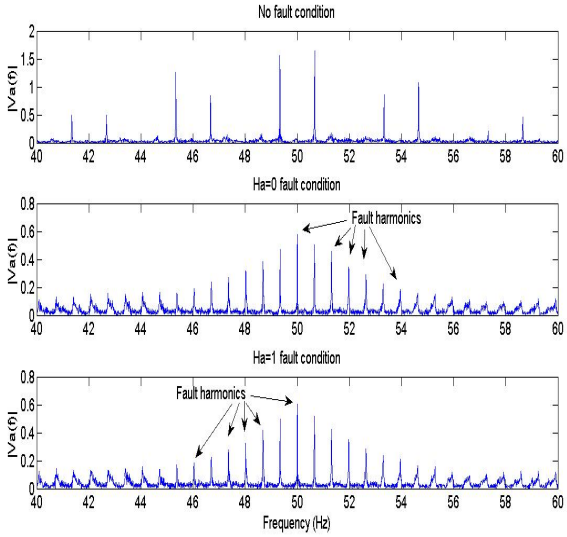

Fig. 8. Amplitude spectrum of phase A line voltage of the BLDC motor

It is possible to distinguish two different fault conditions of Hall Effect sensor by analysing given SED errors of line voltages of the BLDC motor. BLDC motor model is also tested for corresponding position sensor faults of phases B and C. Line voltages of the BLDC motor for various Hall Effect sensor faults are analysed and their SED errors are calculated. Results show that the presented SED errors for corresponding Hall Effect sensor of phase A can also be generalized for the other two position sensors [1].

TABLE IV
SED VALUES FOR $H_a = 0$ FAULT CONDITION

Description	Phase A	Phase B	Phase C
SED before fault $[E_{m-1}(f)]$	957	942	938
SED after fault $[E_m(f)]$	807	1044	1083
SED error $[\varepsilon_m]$	-150	102	145

TABLE V
SED VALUES FOR $H_a = 1$ FAULT CONDITION

Description	Phase A	Phase B	Phase C
SED before fault $[E_{m-1}(f)]$	957	942	938
SED after fault $[E_m(f)]$	1109	925	802
SED error $[\varepsilon_m]$	152	-17	-135

A Hall Effect Identification Flag (HIF) is introduced for each phase of the BLDC motor. Numeric values are assigned to HIF of each phase based on analysing all simulation results and calculated SED errors to identify the faulty sensor. HIF numeric values are assigned as below,

- HIF is set '-1' if SED error is negative;
- HIF is set '1' if SED error is positive.

A multidimensional table is developed for position sensors fault diagnosis based on fault detection and identification flags (HFF and HIF) according to the gathered knowledge from the BLDC motor model behaviour under Hall Effect position

sensor faults. In addition to the simplicity of fault diagnosis method, there is also no need to know exact pattern of the BLDC motor line voltages for different speed and torque loads in advance. Multidimensional knowledge based table for Hall Effect sensor fault diagnosis of the BLDC motor is shown in Table VI [1]. Therefore fault occurrence and fault type are detected as soon as HFF is not zero and faulty sensor is detected based on HIF values of each phase according to the Table VI.

TABLE VI
PROPOSED KNOWLEDGE BASED TABLE FOR POSITION SENSOR FAULTS DIAGNOSIS

Fault type	HIF phase A	HIF phase B	HIF phase C	HFF
No fault	X	X	X	0
$H_A = 0$	-1	1	1	-1
$H_A = 1$	1	-1	-1	1
$H_B = 0$	1	-1	1	-1
$H_B = 1$	-1	1	-1	1
$H_C = 0$	1	1	-1	-1
$H_C = 1$	-1	-1	1	1

IV. EXPERIMENTAL RESULT

The proposed fault diagnosis algorithm of the BLDC motor is investigated through experimental test rig. Low voltage (LV) development board of microchip using PIC18F2431 micro-controller has been modified as shown in Fig. 9 to test the Hall Effect sensor faults of the BLDC motor. Both short circuit and open circuit faults of Hall Effect sensors have been implemented to the experimental BLDC motor and the results are analysed.

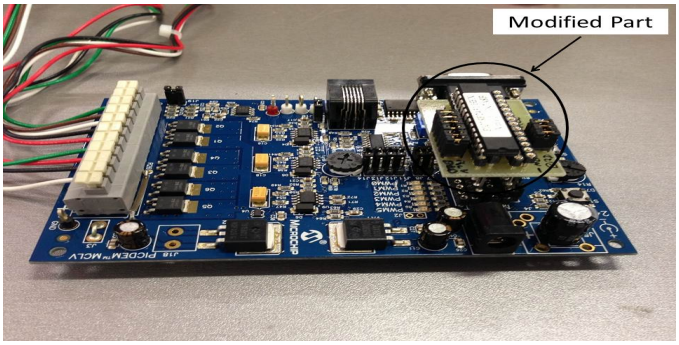

Fig. 9. Modified LV development board of microchip

Open circuit fault of Hall sensor of phase A ($H_a = 0$) is applied to the experimental test motor when the motor was running at 2000 RPM under 0.1 N.m torque load. Speed oscillation and high acoustic noise of the BLDC motor are the first observations after fault occurrence. Line voltages of the experimental BLDC motor under $H_a = 0$ fault condition are shown in Fig. 10. As can be seen pattern of the BLDC motor line voltages are distorted compared to the healthy operating condition. However same as the presented simulation results, the most variations are belong to the phases A and B.

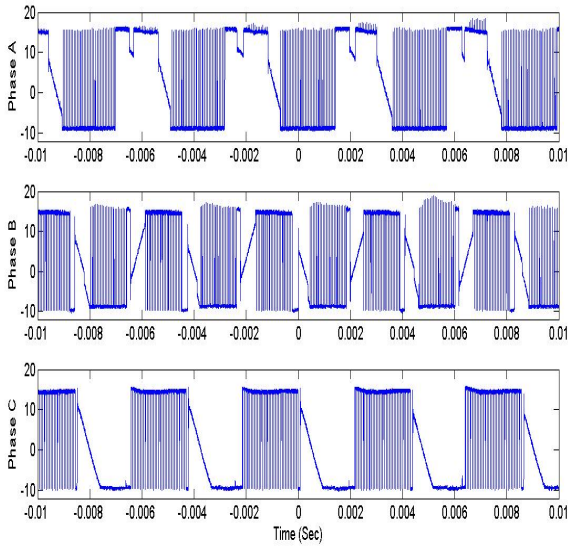

Fig. 10. Line voltages of the experimental BLDC motor during $H_a = 0$ fault condition

Open circuit fault of Hall sensor of phase A ($H_a = 1$) is applied to the experimental test motor when the motor was running at 2000 RPM under 0.1 N.m torque load. Line voltages of the experimental BLDC motor under $H_a = 1$ fault condition are shown in Fig. 11. As can be seen pattern of the line voltages are totally different compared to the $H_a = 0$ fault condition.

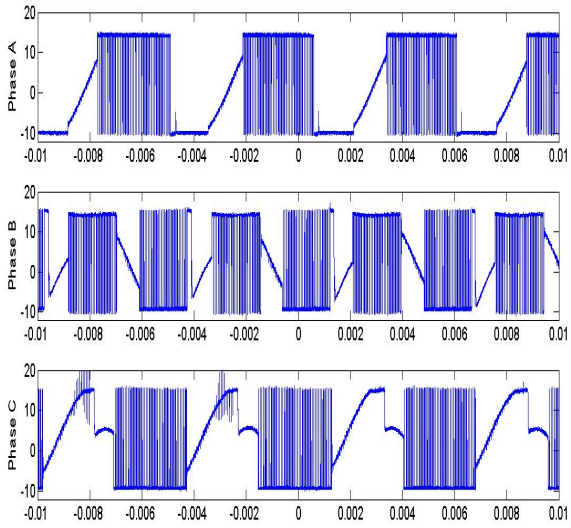

Fig. 11. Line voltages of the experimental BLDC motor during $H_a = 1$ fault condition

As is discussed and presented in Table II, each Hall Effect sensor fault results in loosing specific switching signals of the VSI. Six LED lights are implemented on the control board to show the status of the switching signals. If the switching signal is zero, then the corresponding LED light is turned off and

vice versa. Status of the LED lights for open circuit and short circuit faults of the Hall Effect sensor of phase A are shown in Fig. 12. As can be seen switching signals PWM_1 and PWM_4 for open circuit fault condition and switching signals PWM_0 and PWM_5 for short circuit fault condition are zero. Therefore effects of Hall Effect sensor faults on switching signals of the VSI that are presented in Table II are validated through experiment.

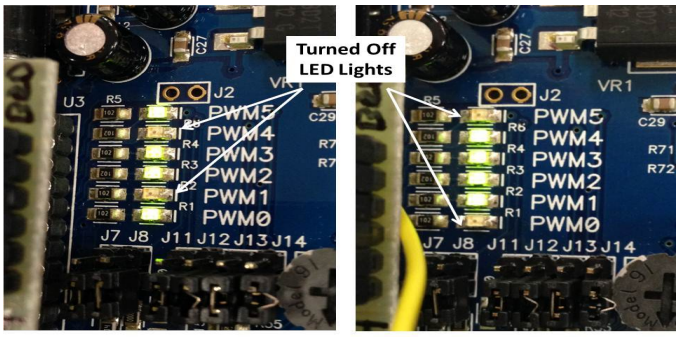

(a) Ha=0 Fault condition (b) Ha=1 Fault condition

Fig. 12. Status of switching LED lights on the control board under position sensor faults of phase A: (a) Open circuit fault (b) Short circuit fault

Single-sided amplitude spectrum of phase A line voltages of the experimental BLDC motor under no fault, Hall Effect sensor open circuit fault ($H_a = 0$) and Hall Effect sensor short circuit fault ($H_a = 1$) conditions are plotted in Fig. 13. As can be seen same as the case in simulation results, high amplitude harmonics are added to the line voltage of phase A of the experimental BLDC motor under Hall Effect sensor fault conditions. Therefore spectral energy densities of the line voltages are not same for different position sensor faults in the BLDC motor drive.

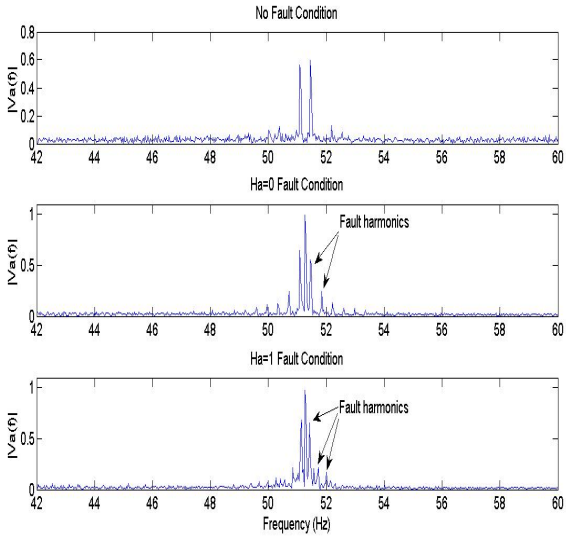

Fig. 13. Amplitude spectrum of phase A line voltage of the BLDC motor

Spectral energy density errors of the experimental BLDC motor line voltages under $H_a = 0$ and $H_a = 1$ fault conditions are calculated and given in Tables VII and VIII. As can be seen the assigned numeric values to the Hall Effect identification flag based on practical SED errors is as same as the simulation ones presented in Tables IV and V. The experimental SED errors are not as large values as the simulation SED errors due to the inbuilt over current protection circuit of the controller board.

TABLE VII
SED VALUES FOR EXPERIMENTAL $H_a = 0$ FAULT CONDITION

Description	Phase A	Phase B	Phase C
SED before fault $[E_{m-1}(f)]$	314.9870	322.1711	322.3580
SED after fault $[E_m(f)]$	301.1294	329.6414	369.2658
SED error $[\varepsilon_m]$	-13.8576	7.4703	46.9078

TABLE VIII
SED VALUES FOR EXPERIMENTAL $H_a = 1$ FAULT CONDITION

Description	Phase A	Phase B	Phase C
SED before fault $[E_{m-1}(f)]$	314.9870	322.1711	322.3580
SED after fault $[E_m(f)]$	330.2032	319.5225	310.2840
SED error $[\varepsilon_m]$	15.2162	-2.6486	-12.074

The low voltage experimental BLDC motor is also tested under open circuit and short circuit faults of the other Hall Effect sensors, corresponding sensors of phase B and C, and their experimental results are analysed. Calculated experimental SED errors of the line voltages prove the fault diagnosis algorithm and validate the knowledge based fault identification table, Table VI, developed through the simulation model.

V. REMEDIAL STRATEGY

The Faulty Hall Effect sensor must be isolated and its signal should be disconnected from the BLDC motor controller. A simple technique is proposed to generate the Hall Effect signal of the faulty sensor by micro-controller. In this technique, corresponding commutation signal of the faulty sensor is generated by implementing 120 electrical degree delays to one of the other two available Hall Effect sensors. A simple equation has been introduced to calculate the time that is needed for the BLDC motor rotor to pass one electrical degree [3]. If the BLDC motor speed does not change during commutation intervals (it is assumed that the controller keeps the motor speed constant), the time of one electrical degree rotation of the BLDC motor can be calculated by (5), where P is the pole numbers and ω_{ref} is the reference speed of the motor in RPM. Effectiveness of the proposed technique to calculate the correct time delays and generate the correct commutation signals in the BLDC motors is proved through simulation and experiment [3].

$$t = \frac{1}{\frac{P}{2}(6 * \omega_{ref})} \tag{5}$$

An embedded code is written and implemented in Simulink model of the BLDC motor to test performance of the proposed FTCS. Open circuit fault $H_a = 0$ is applied to the simulation model at $t = 0.5$ s while the motor is running at 2000 RPM

under 0.1 N.m torque load. Speed characteristics of the BLDC motor with the implemented fault tolerant control system is shown in Fig. 14.

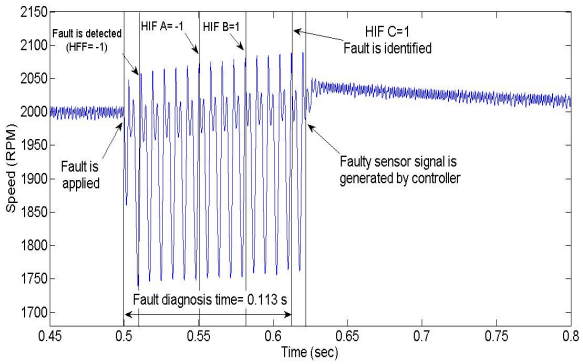

Fig. 14. Speed response of the fault tolerant controlled BLDC motor drive

Fault is detected, identified through calculating HFF and HIF of each phase. Fault diagnosis time in simulation model is about 0.113 second which is quite fast and acceptable for motor drives. Faulty sensor signal are generated by the controller that maintains the proper performance of the BLDC motor in the post-fault condition. Simulation results show effectiveness of the proposed remedial strategy for Hall Effect sensors breakdown in the BLDC motors.

VI. Conclusion

In this paper, a fault tolerant control system for Hall Effect position sensors failure in the BLDC motor drives is presented. Behaviour of the BLDC motor is analysed under various position sensor faults conditions through a validated simulation model. It is shown that any position sensor faults effect directly on the applied line voltages of the BLDC motor. Fault occurrence is detected through Hall Effect sensor signals analysis. A knowledge based table is developed to identify the faulty sensor based on DFT analysis of the BLDC motor line voltages. Since faulty sensor is identified through spectral density errors of the line voltages of the motor; the exact pre-knowledge of line voltages pattern under various working condition is not needed. This advantage of the proposed FTCS makes it useful for application with frequent change of speed and load torque such as electric vehicles. A simple technique is proposed to generate the signal of faulty sensor by implementing the time delays between Hall Effect sensor signals in post-fault condition. Effectiveness of the proposed fault diagnosis algorithm and the proposed knowledge based table for Hall Effect sensors breakdown are investigated and discussed through experiments. Correctness of the proposed fault diagnosis algorithm is proved by the experimental results.

References

[1] A. Tashakori and M. Ektesabi, "A simple fault tolerant control system for hall effect sensors failure of bldc motor," in *Proceeding of the 8th IEEE Conference on Industrial Electronics and Applications (ICIEA 2013)*, (Melbourne, VIC), pp. 1011–1016, 2013.

[2] T.-H. Kim and M. Ehsani, "Sensorless control of the bldc motors from near-zero to high speeds," *IEEE Transactions on Power Electronics*, vol. 19, no. 6, pp. 1635–1645, 2004.

[3] A. Tashakori and M. Ektesabi, "Stability analysis of sensorless bldc motor drive using digital pwm technique for electric vehicles," in *Proceeding of 38th Annual Conference on IEEE Industrial Electronics Society, IECON 2012*, pp. 4898–4903, October 2012.

[4] A. Tashakori and M. Ektesabi, "Fault diagnosis of in-wheel bldc motor drive for electric vehicle application," in *In proceeding of the 2013 IEEE Intelligent Vehicles Symposium*, (Gold Coast, Australia), pp. 925–930, June 23-26 2013.

[5] X.-Q. Liu, H.-Y. Zhang, J. Liu, and J. Yang, "Fault detection and diagnosis of permanent-magnet dc motor based on parameter estimation and neural network," *IEEE Transactions on Industrial Electronics*, vol. 47, no. 5, pp. 1021–1030, 2000.

[6] Z. Wang, R. Schittenhelm, M. Borsdorf, and S. Rinderknecht, "Application of augmented observer for fault diagnosis in rotor systems," *Engineering Letters*, vol. 21, no. 1, pp. 10–17, 2013.

[7] S. Mondal, G. Chakraborty, and K. Bhattacharyya, "Unknown input high gain observer for fault detection and isolation of uncertain systems," *Engineering Letters*, vol. 17, no. 2, pp. 121–127, 2009.

[8] E. Balaban, A. Saxena, P. Bansal, K. Goebel, and S. Curran, "Modeling, detection, and disambiguation of sensor faults for aerospace applications," *IEEE Sensors Journal*, vol. 9, no. 12, pp. 1907–1917, 2009.

[9] N. B. Samoylenko, Q. C. Han, and J. Jatskevich, "Dynamic performance of brushless dc motors with unbalanced hall sensors," *IEEE Transactions on Energy Conversion*, vol. 23, no. 3, pp. 752–763, 2008.

[10] Y.-S. Jeong, S.-K. Sul, S. Schulz, and N. Patel, "Fault detection and fault-tolerant control of interior permanent-magnet motor drive system for electric vehicle," *IEEE Transactions on Industry Applications*, vol. 41, no. 1, pp. 46–51, 2005.

[11] L. Wang, J. Liu, and X. Wu, "Fault analysis on driving motors of lunar rover wheels," in *Proceeding of the International Conference on Electrical Machines and Systems, ICEMS 2011*, (Beijing, China), Aug 2011.